Biophys. Struct. Mechanism 4, 67–85 (1978)

Biophysics of Structure and Mechanism

The Heterogenious Solubility of Oxygen in Aqueous Lecithin Dispersions and its Relation to Chain Mobility

A NMR Relaxation and Wide-Line Study*

A. Peters and R. Kimmich

Universität Ulm, Sektion Kernresonanzspektroskopie,
Postfach 4066, D-7900 Ulm/Donau, Federal Republic of Germany

Abstract. A method is described that allows to determine the oxygen concentration in microscopic subphases, such as lipid bilayers, by measuring the enhancement of NMR spin-lattice relaxation (T_1) caused by paramagnetic oxygen. The presence of oxygen itself provides the measuring effect, which has the advantage of the lack of any distortions by large probe molecules in the system. The T_1-jump of the water protons of a dipalmitoyl lecithin (DPL)/water-dispersion at the phase transition yields information about the O_2-solubility in the DPL bilayers.

The results can be interpreted in a straightforward way in terms of a two phase model DPL/H_2O. The measurements indicate, however, that a more appropriate approach is possible if a three-phase system DPL/bound water/free water is taken into account. The O_2-partition coefficients and the free enthalpies of solution are evaluated for all subsystems in both models.

The oxygen solubility in paraffin chains is obviously connected to the defect structure. A comparison is drawn between n-paraffins and the DPL fatty-acid chains. The gel-state of DPL lamellae does not correspond to the crystalline paraffin state, but rather to the more disordered rotator-phase. To emphasize this, NMR second moment data of DPL and some n-alkanes are compared.

Key words: Oxygen-Solubility – Lipid bilayers – NMR relaxation – Defect structure – NMR second moment.

I. Introduction

Phospholipids, and of this group mainly lecithins have been found to form stable lamellar structures, not only in natural membranes, but also in aqueous dispersions of synthetic molecules. Natural and synthetic lecithins exhibit the well-known gel to liquid crystalline phase-transition, which changes the defect structure of the bilayer

* Reported in part on the VIIth International Conference on Magnetic Resonance in Biological Systems, St. Jovite, Canada, September 19–24, 1976

(Träuble and Eibl, 1975) but preserves the lamellar arrangement of the molecules.

It is rather plausible that the defect structure within the lamellae determines the solubility of small dissolved molecules. Thus, being interested in the passive transport properties across lipid bilayers, we have to deal with the solubility of appropriate molecules in such systems, and as a further basic aspect, with the type and mobility of defects in the lipid hydrocarbon chains.

This defect structure can be discussed on the basis of gauche/trans sequences of the carbon-carbon bonds, leading to special types of defects defined as kinks (Pechhold, 1968). Recently a number of papers appeared using the kink concept to describe lipid bilayers in the liquid-crystalline as well as in the gel state (Träuble, 1971, 1972; Seelig and Seelig, 1974; Horwitz et al., 1972; Kimmich and Peters, 1975; Jackson, 1976). In previous papers we have especially discussed the question whether these chain defects are able to diffuse along the chains and which experimental consequences should be expected thereof (Kimmich and Peters, 1975; Kimmich, 1976).

In this paper we will add some arguments from NMR wideline properties in order to give an idea of the extent of the chain mobility in dependence on the temperature. On the other hand we have investigated the solubility of oxygen in dipalmitoyl lecithin (DPL) bilayers as one example out of a class of molecules able to permeate through membranes. The choice has fallen to oxygen for several reasons: Oxygen is biologically relevant, electrically neutral and sufficiently small to fit into kink vacancies. Furthermore, it is electron paramagnetic, allowing to detect the local concentration by the NMR-method described below in detail.

A proton spin in a system containing only protons and electron paramagnetic oxygen as dipole particles can be flipped from one orientation to the other by dipolar interaction with other protons and additionally with oxygen molecules. Thus the presence of oxygen causes a relaxation enhancement, provided that material or spin-diffusional exchange to all observed protons is rapid compared to the relaxation times (Zimmerman and Brittin, 1957). Designating the proton relaxation rate (i.e. the reciprocal longitudinal relaxation time T_1) due to the interaction with the oxygen molecules by R and that one due to the interaction with other protons by R_{dia}, we obtain for the effective rate in a system containing oxygen

$$R_{tot} = R + R_{dia} . \tag{1}$$

R_{dia} can be measured in a sample free of oxygen, while R_{tot} is the rate detected in a sample with applied oxygen pressure. Measuring R_{dia} and R_{tot} allows to derive R, which is of final interest because this rate is proportional to the oxygen concentration. Therefore, the following discussion concerns predominantly the quantity R. Generally it holds (Bloembergen et al., 1948).

$$R = F \cdot c , \tag{2}$$

where c is the oxygen concentration and F is a factor containing among some constants the sum of intensity functions relevant for this relaxation process. To evaluate the oxygen concentration from Equation 2, we must know the factor F, which requires a special procedure described below. It should be mentioned that F

principally depends on experimental conditions such as temperature and magnetic field strength as well as on structural details of the system under investigation.

First measurements performed under this aspect (Kimmich and Peters, 1975) approached the problem by evaluating the paramagnetic relaxation rate R^L of the fatty acid residues in a DPL-D_2O-dispersion at several temperatures

a) in dependence on oxygen pressure (at constant Larmor frequency) and

b) in dependence on Larmor frequency (at constant pressure),

yielding the following conclusions:

a) R^L is proportional to the external oxygen pressure. This shows that Henry's law is valid for the interior of the lecithin lamellae up to 80 bar. The fact that considerable amounts of oxygen are also solved in the gel state below the phase transition, in contrast to crystalline paraffins, suggests that the term "crystalline" should be used only in a very limited sense for the gel state of DPL-bilayers.

b) The frequency-dependence of R^L has to be interpreted discriminatively: Above the phase transition, the measurements can be described by a simple Poisson process with one single correlation time. Below the transition, the curves are too flat to be fitted by a single Poisson process. Thus, the factor F is basically altered when passing the phase transition. Therefore, it was not possible to derive the absolute concentration in the two phases nor to evaluate its relative alteration at the phase transition from these experimental data alone.

The observation that the equilibrium values of R^L are reached very slowly, because the transport of oxygen through the water phase to or from the bilayers is diffusion controled, however, allowed to estimate the change in O_2-concentration at the phase transition[1]. We now want to report a modified procedure yielding more accurate absolute values of the oxygen concentration in microscopic subphases such as DPL-bilayers.

II. The Method

Fundamentally, we take advantage of the fact that the connection between oxygen concentration, partial pressure and the relaxation rate is very well known for water (Hausser and Noack, 1965). The detection of the water relaxation rates of a DPL-dispersion, when passing the phase transition, will give us information about the situation within the DPL-bilayers.

In DPL/D_2O-dispersions, relaxation rates can be obtained for both the DPL and the water phase by measuring separately the proton and the deuterium relaxation. Alternatively, the water relaxation can be detected in a DPL/H_2O-dispersion by analyzing the proton FID into a wide-line part arising from the DPL-bilayers and a motionally narrowed signal of the water, Figure 1. (It should be noted that, as a consequence of the rapid exchange compared with relaxation times, not only the free but also the hydration water yields a FID decaying much slowlier than that of the DPL-bilayers. This can be demonstrated by comparison with a DPL/D_2O sample.)

---

[1] "Phase transition" always should be read as main transition of the DPL-bilayers. At the so-called pre-transition (Hinz and Sturtevant, 1972) no abrupt change in the oxygen concentration in the lecithin bilayers could be detected

The second method is more sensitive and allows the rapid detection of the water signal with one single FID. Therefore all reported results have been obtained with this procedure.

The interpretation presented below depends on the assumption that the alkane proton relaxation is enhanced only by the oxygen within the lamellae while the water relaxation is solely influenced by oxygen dissolved in the water phase itself. This

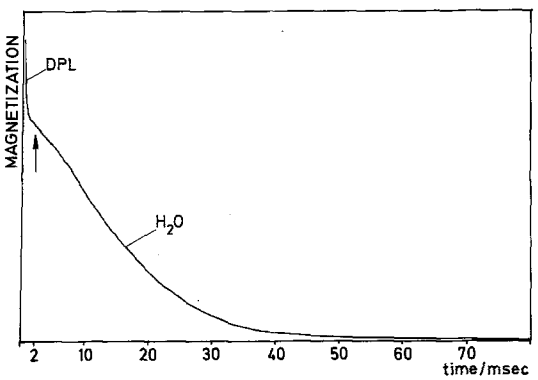

Fig. 1. The free induction decay of ^1H in a DPL/H_2O dispersion following a $\pi/2$-RF-pulse is a superposition of a rapid decay from the DPL and a slow decay from the motionally narrowed water. After about 2 ms (point indicated by an arrow) the FID amplitude is practically produced by H_2O protons alone. T_1 plots of the amplitudes measured at this point are purely exponential and solely reflect the relaxation of the water protons

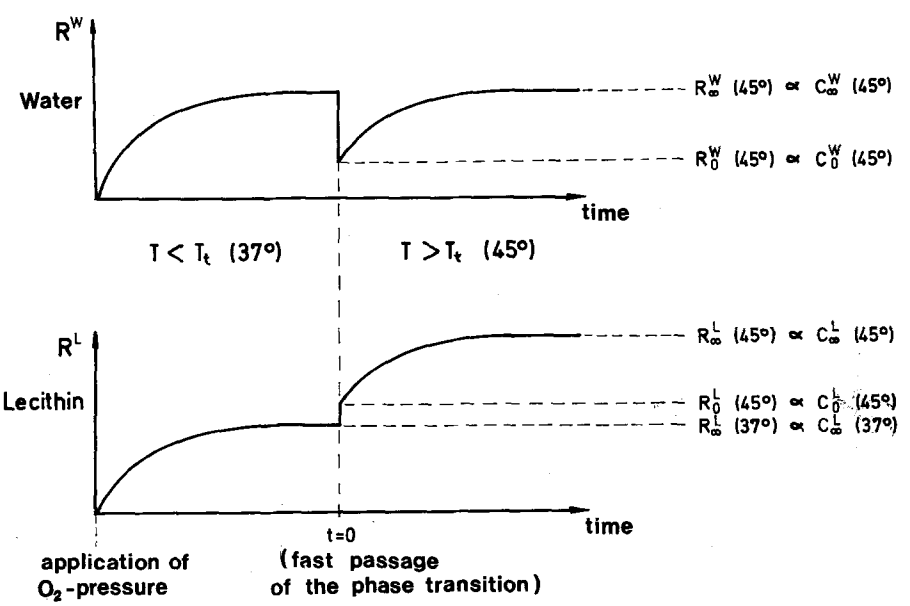

Fig. 2. Schematical illustration of the process of oxygen concentrations and proton paramagnetic relaxation rates according to the measuring program described in the text

assumption is strongly supported by the following arguments (Kimmich and Peters, 1975):

The number of water molecules incorporated within the lamellae must be extremely small compared to the water phase itself, keeping in mind that no hydrogen bonds can be expected in the DPL phase.

The water and the hydrophobic phase of the fatty acid residues are separated by layers containing no protons and therefore preventing any spin diffusion between both phases.

It will be shown below that the results obtained from the water relaxation are complementary to results derivable from the DPL relaxation.

Finally, it should be mentioned that the effective relaxation rates of the DPL hydrocarbon protons and those of the water are different and behave quite independently. The gel-to-liquid-crystal phase transition *increases* the equilibrium oxygen concentration within the bilayers and consequently the relaxation rate of this phase, while that of the water shows a *decreasing* tendency as expected from the normal temperature behaviour.

As an illustration we show in Figure 2 the qualitative time evolution of the relaxation rates both in the water and in the DPL-bilayers after applying the external oxygen pressure and passing the phase transition some time later. The initial rise in the relaxation rates is determined by the diffusion of oxygen from the gas space to the interior of the water volume and from there into the DPL-bilayers. After ca. 20 days the equilibrium is reached. Now heating over the phase transition point of the DPL within ca. 4 min leads to a sudden nonequilibrium: oxygen spontaneously flows from the water into the lamellae, causing a reduction of the relaxation rate of the water and an increase of that of the DPL-bilayers. The new equilibrium will be reached only after a sufficient amount of oxygen has diffused from the gas space into the water to replace the lacking amount of gas. These complementary concentration changes at the phase transition allow the calibration of Equation 2 for temperatures just near the phase transition, because the alterations of the oxygen concentration in the water can be calculated from changes in the water relaxation rate according to the well known factor $F(H_2O)$ of Equation 2 (Hausser and Noack, 1965).

It should be noticed in this context that the proportionality factor F for DPL-protons changes at the phase transition, so that it is essential to use the water relaxation rates to calibrate indirectly Equation 2 for DPL.

III. Evaluation Formulae for the Single Water-Phase Model

In the following we will use two different approaches. In a first evaluation a single water phase will be assumed, and hydration effects will be discussed later. For the abbreviations in the subsequent equations, we shall use two indices: the lower index of the rates and concentrations refers to the time for which they have been evaluated: "0" refers to the time immediately after having passed the phase transition, "∞" to the time when the system has reached equilibrium. The upper index of each quantity refers to the system: "L" stands for DPL, "W" for water. The temperatures at which

the measurements have been performed[2] are 37° C and 45° C, these temperatures will be given in brackets together with the DPL/water mass ratio. Examples are:

$C^L_\infty(37)$: Equilibrium concentration of oxygen in the DPL-lamellae at 37° C.

$C^w_0(45)$: Concentration of oxygen in the water just after having passed the phase transition.

$C^w_\infty(45)$: Equilibrium concentration of oxygen in the water at 45° C.

Furthermore, we define:

ΔC_I: abrupt change of O_2-concentration when passing the phase transition

ΔC_{II}: change of O_2-concentration by renewed attainment of the equilibrium of solvation above the phase transition.

The fundamental equation of the following treatment states that the partition coefficient K for oxygen between DPL and water at a given temperature does not depend on the quantity of oxygen at disposal, nor on the DPL/water mass ratio:

$$K(45) = K_0(45) = K_\infty(45)\,, \tag{3}$$

where

$$K_0(45) = \frac{C^L_\infty(37) + \Delta C^L_I}{C^w_0(45)}\,; \quad K_\infty(45) = \frac{C^L_\infty(37) + \Delta C^L_I + \Delta C^L_{II}}{C^w_\infty(45)}. \tag{3a, b}$$

The physical reason for the validity of Equation 3 is that the exchange of oxygen between DPL and water is rapid compared with the diffusion processes within the water. Below, we shall need a quantity which could be called "jump-quotient":

$$S = \frac{C^w_0(45)}{C^w_\infty(37)} = \frac{R^w_0(45)}{R^w_\infty(37)} < 1, \tag{4}$$

where we have assumed that the factor F of Equation 2 remains constant. This quantity S is the basic variable to be measured.

Let us now calculate the O_2-concentration jump in the DPL-membranes ΔC^L_I: As the changes of oxygen amount in the water and in the bilayers at the phase-transition are equal, we can write

$$\Delta C^L_I \cdot m_L = \Delta C^w_I \cdot m_w \tag{5}$$

(m_L, m_w: masses of DPL and water, respectively).

ΔC^w_I can be expressed by

$$\Delta C^w_I = C^w_\infty(37) \cdot (1 - S) \cdot M\,, \text{ where } M = \frac{m_w}{m_L}. \tag{6}$$

We now consider two DPL/water mass ratios designated by α and β. Because of

$$K_0(45, \alpha) = K_0(45, \beta)$$

we find, by combining Equations 3a, 4 and 6 for both mass ratios:

$$K(37) = \frac{C^L_\infty(37)}{C^w_\infty(37)} = \frac{M_\beta S_\alpha (1 - S_\beta) - M_\alpha S_\beta (1 - S_\alpha)}{S_\beta - S_\alpha}. \tag{7}$$

[2] Both temperatures have been chosen close to the main transition in order to minimize any alteration of the oxygen solubility in the water phase during the temperature jump, and in order to allow a rapid passage of the phase transition. 37° C lies between the pre-transition and the main-transition. Nevertheless the results obtained for the DPL bilayers are also relevant for the general gel phase according to our previous results (compare footnote 1)

Analogously, we find from

$$K_0(45) = K_\infty(45)$$

by the use of Equations 3a, b and 7

$$K(45) = \frac{C^L_\infty(45)}{C^W_\infty(45)} = \frac{M_\beta(1 - S_\beta) - M_\alpha(1 - S_\alpha)}{S_\beta - S_\alpha}. \tag{8}$$

Equations 7 and 8 depend only on $M_{\alpha,\beta}$ and $S_{\alpha,\beta}$, enabling us to derive $K(37)$ and $K(45)$ by measuring these values for two DPL/water mass ratios α and β.

IV. Apparatus, Samples and Measurements

All relaxation measurements were carried out with a Bruker SXP 4-100 spectrometer, at a Larmor frequency of 90 MHz, using a Bruker B-E 38 shimmed high resolution magnet system. The FIDs were recorded on a Bruker B-C 104 transient recorder. The measurements of the relaxation rates were performed by the π-τ-$\pi/2$-method. To enable a sufficient gas concentration in the samples, special high pressure glass tubes were used (Kimmich and Peters, 1975).

The samples were produced by ultrasonically dispersing 7% dipalmitoyl lecithin (Fluka) in water at 50° C and then evaporating down to the desired concentration, as previously described (Kimmich and Peters, 1975). The water used in these investigations was triple distilled using quartz containers. The final sample contained 100 mMol NaCl per liter to stabilize the lamellae. Two different concentrations with 53% and 29% DPL (w/w) were used. These concentrations were determined by weighing a part of the sample, evaporating at 10^{-4} torr for two days to remove the bulk water and subsequently drying over P_2O_5 for one week. The weight of the dry DPL determined after this time could not be reduced by prolonged drying periods. This procedure was repeated after the measurements in order to control whether any water had evaporated during the long measuring cycles. The purity of the lecithin was checked before and after the whole procedure by thin layer chromatography and high-resolution nmr (dissolved in $CDCl_3$). No decomposition of the material could be detected.

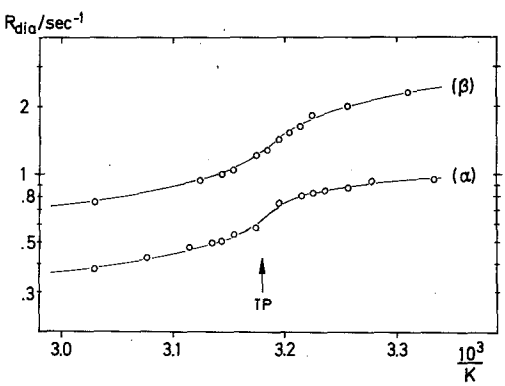

Fig. 3. Temperature dependence of the diamagnetic relaxation rates of the water protons in DPL/H_2O-dispersions containing 29% (α) and 53% DPL (β). TP denotes the temperature of the gel to liquid-crystalline phase transition of the DPL

Before applying the O_2-pressure, the diamagnetic relaxation rates were determined at several temperatures below and above the transition point. All water relaxation curves turned out to be purely exponential. The data are given in Figure 3. Evidently, the relaxation rates differ by a factor of about 2, where R_{dia} is lower in the higher water concentration. The explanation thereof is connected with the hydration shell of the polar head groups of the lecithin. In this hydration water, molecular

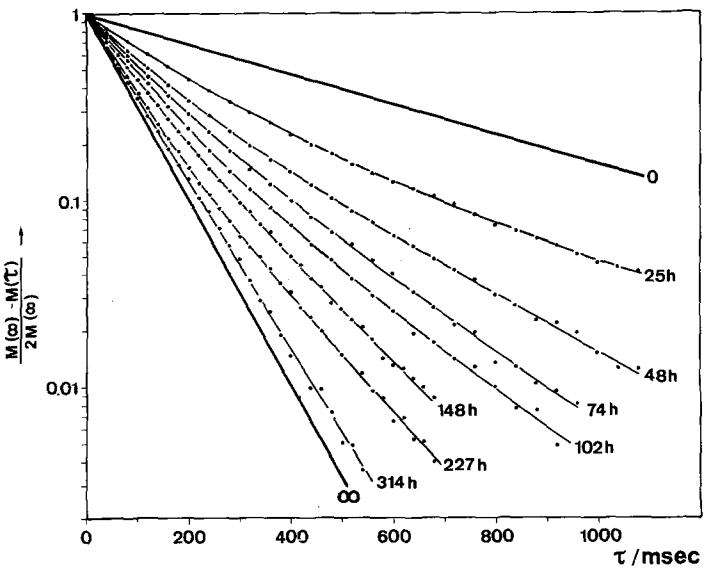

Fig. 4. Relaxation plots for the water protons in the 53% DPL/H_2O dispersion at various times after the application of an oxygen pressure of 55 bar. Before the application ($t = 0$) and in the case of equilibrium of solvation ($t = \infty$), the curves are exponential. At intermediate times nonexponential plots are measured, indicating a distribution of oxygen concentrations due to the slow diffusion of O_2 through the sample

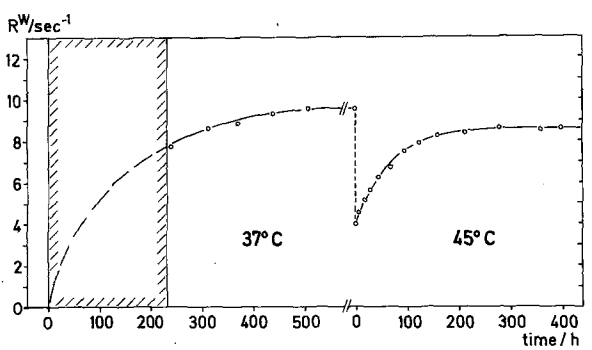

Fig. 5. Paramagnetic water proton relaxation rates for sample β, to be compared with the schematic illustration Figure 2. In the hatched area, nonexponential relaxation occurs according to Figure 4. At 45° C, the deviation from the exponential behaviour of the intermediate relaxation plots is essentially smaller and is not resolved by our measurements

Table 1

			Temperature	Sample α	Sample β
Mass ratio	$M = \frac{m_w}{m_L}$			2.44	0.885
Relaxation rates	R^w_{dia}	$[s^{-1}]$	37° C	0.83	1.79
			45° C	0.50	1.00
	$R^w_{\infty,\,tot}$	$[s^{-1}]$	37° C	8.70	11.4
			45° C	7.69	9.80
	R^w_∞	$[s^{-1}]$	37° C	7.86	9.58
			45° C	7.19	8.80
	R^w_0	$[s^{-1}]$	45° C	4.50	4.00
Jump quotient S				0.572	0.418

motion and arrangement is different from the free water, leading to a distribution of relaxation rates, but as the material exchange is fast between the different environments, we nevertheless measure exponential relaxation slopes exhibiting a single average relaxation time. These facts have been investigated in detail by Gottlieb et al., 1973.

After the measurements on the diamagnetic samples have been performed, an oxygen pressure of 55 ± 2 bar was applied and the relaxation behaviour was watched until reaching equilibrium. Far from equilibrium, no exponential T_1-plots could be observed because of the inhomogeneity of the O_2-concentration within the sample (Fig. 4). Since convection does not take place as a consequence of the high viscosity of the dispersion, the experiments were rather lengthy: for each sample, the measurements took about 40 days. In Figure 5, we have plotted the H_2O-relaxation rates, which correspond to the development of the O_2-concentration, as schematically given in Figure 2. In both samples the phase transition is accompanied by a sharp decrease in R, i.e. the partition coefficient rises discontinuously.

All experimental data, as referred to in section V and VI, are listed in Table 1.

V. Results for the Single Water-Phase Model and Controls

For the values given in Table 1 and with Equations 7 and 8 we obtain for the partition coefficients:

$$\boxed{\begin{aligned} K(37) &= 0.9 \pm 0.3 \\ K(45) &= 3.4 \pm 0.5 \end{aligned}}$$

These results simply express that below the phase transition the solubility of oxygen in the lamellae is about the same as in water, above the transition it is 3 . . 4 times higher. Keeping in mind that the partition coefficient reflects nothing else than the difference in the free enthalpies of solution ΔG for O_2 between the aqueous and the lipid phase,

$$K(T) = \exp\{-\Delta G(T)/RT\}, \tag{9}$$

we can evaluate ΔG as

$$\begin{array}{l} \Delta G(37) = +0.05 \pm 0.2 \text{ kcal/Mol} \quad (+0.27 \pm 0.8 \text{ kJ/Mol}) \\ \Delta G(45) = -0.80 \pm 0.15 \text{ kcal/Mol} \quad (-3.23 \pm 0.6 \text{ kJ/Mol}) \end{array}$$

Examining the experimental data in Table 1 we notice that there is a difference between $R_\infty^w(37)$ and $R_\infty^w(45)$ of about 9% in both samples. By extrapolation, we find that Henry's constant will fall by about 8% between these two temperatures (d'Ans and Lax, 1967). So the T_1-alteration is solely due to the difference in the O_2-solubilities. This fact is very important: it means that the factor F in Equation 2 remains constant for the water as required for the validity of Equation 4. The jump-factor S, defined by Equation 4, is not affected by this alteration of Henry's constant, because S only reflects the decrease of the momentaneous concentration in the water, i.e. of the equilibrium oxygen concentration at 37° C.

The second interesting point is that the R_∞^w-values differ from one DPL/water mass-ratio to the other by about a factor 1.22 at both temperatures. This means, that the average sum of intensity functions and/or the average oxygen concentration in free and bound water are different. In fact, we have to consider a different Henry-constant for the hydration water, leading to a tertiary system with respect to the O_2-solubility. Therefore, the values given for K and ΔG have to be considered as averages of two different ratios of free to bound water. A corrective calculation will be discussed below, which will lead to the solubility parameters of all three subsystems, at the expense of some further assumptions.

To consolidate our interpretations, we have repeated the measurements for the DPL-protons in DPL-D_2O-dispersions of the same mass ratios. These measurements show a behaviour complementary to that of the water relaxation. As men-

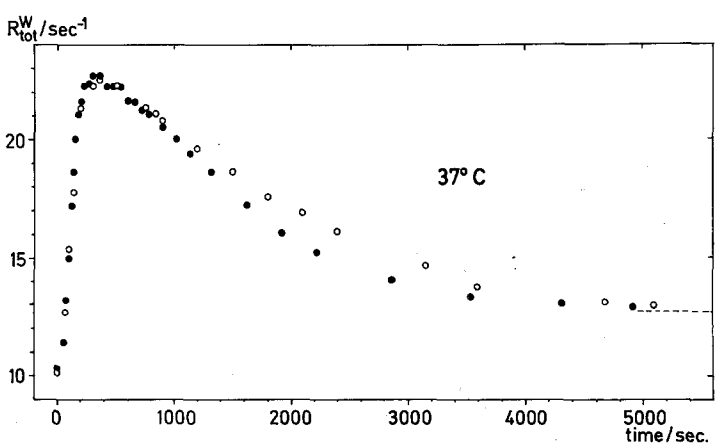

Fig. 6. Time evolution of the total water-proton relaxation rate for sample β exposed to an O_2-pressure of 55 bar, when, after having reached the equilibrium of O_2-solvation above the DPL phase transition, the temperature is again lowered beneath the transition point. (○ ●: two successive measurements)

tioned above, the jump factors S for the DPL-protons cannot be evaluated because of the alteration of the intensity functions (Kimmich and Peters, 1975). The quantity $\Delta C^L_{II}(\alpha)/\Delta C^L_{II}(\beta)$, measured at the fixed temperature of 45° C (see Eq. 3b and Fig. 2), however, is suitable as a control. This ratio was found to be compatible with the results derived from the water relaxation, although the errors of measurement are very much higher in this case because of non-exponential relaxation plots for the DPL-protons. These curves were separated into two exponential decays by computer aid (compare Kimmich and Peters, 1975).

The experiment has also been performed in the reverse direction by passing the phase transition from 45° C to 37° C, i.e. oxygen will be pressed out of the lamellae into the water. In Figure 6, this is shown for the 53% sample (β). During the first four minutes after the temperature control is set to the lower value, the phase transition takes place and we notice that R^w is raised continuously, indicating that the O_2-concentration in the water has risen. Afterwards, a concurrent process lowers R^w again with a time constant of about 20 min, which can be interpreted by the slow dissolution of oxygen into microscopic gas bubbles. It is remarkable, however, that the new equilibrium value of R^w at 37° C stabilizes itself at a value which is about 12% higher than in the initial experiment. Incidentally, stable supersaturated solutions of O_2 in water are a well known phenomenon (Dost, 1906; Metschl, 1924). Because of the fast T_1-alterations, the measurements in Figure 6 have been performed by means of the π-τ-$\pi/2$-Null-method, which allows very fast T_1-measurements with satisfactory accuracy, provided that the relaxation is exponential. If we extrapolate the falling part of the curve to time 0, we obtain a new jump quotient S^* for the oxygen withdrawn from the lecithin:

$$S^* = \frac{C^w_\infty(45)}{C^w_0(37)} = \frac{R^w_\infty(45)}{R^w_0(37)} < 1. \tag{10}$$

Using Equations 3 and 6, we derive

$$S^*_\beta = \frac{K(37) + M_\beta}{K(45) + M_\beta} = S_\beta . \tag{11}$$

From the measurements, we find $S^*_\beta = 0.4 \,..\, 0.41$, which agrees very well with S_β from Table 1.

Raising the temperature above the transition once more again yielded the same behaviour as in our initial experiment and the same jump quotient could be found.

Parallel to the T_1-change at the transition from the liquid-crystalline state to the gel phase, a considerable shortening of the free induction decay time of the water has been observed, which means that the NMR-line has drastically broadened (Fig. 7). Raising the temperature again, the broadening recedes. The line-broadening temporally coincides with the formation of the gas bubbles, discussed above. When the induction decay time has reached its minimum, the surplus oxygen, squeezed from the lamellae, has already disappeared from the water protons, as evident from the T_1 values of the water. We have also measured the transverse relaxation rates of the water with Carr-Purcell-Meiboom-Gill sequences and found that in all cases T_2 is not essentially shorter than T_1. Thus the observed broadening cannot have its origin

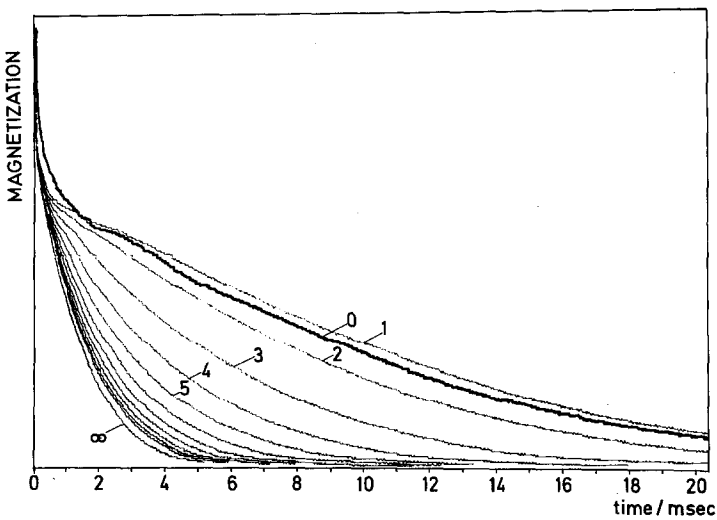

Fig. 7. The proton free induction decays of a DPL/H_2O dispersion under 55 bar of O_2-pressure exhibit the deletion of field homogeneity by the formation of gas bubbles in the sample. The bold drawn FID No. 0 has been taken for the totally equilibrated sample at 45° C. After switching down the temperature to 37° C, the DPL phase transition takes place within about 4 min. After this time, the FID No. 1 was recorded. All following FIDs have been recorded after successive time intervals of 200 s. The FID No. ∞ represents the equilibrium decay, the constancy of which has been controled over a period of one month. When the temperature is raised to 45° C again, the same course of FIDs occurs with the opposite drift direction

in an extreme relaxation enhancement, but must be due to a strong disturbance of the overall field homogeneity in the sample. Now it is a well known fact that small particles suspended in a material of different magnetic susceptibility lead to distortions of the local field. So the formation of gas bubbles in the sample is manifested hereby. We must remark that this phenomenon also occurs in pure water: a cloud of fine bubbles appears, when high oxygen pressure is suddenly reduced on a saturated water sample (Clare, 1925). In similar experiments, the colloidal nature of such dispersions ["gas-liquid sols"] has been demonstrated (Andreev and Kulikova, 1935; Krause and Kapitańczyk, 1935).

VI. Extention to two Water Phases

In this section an improved model is given, taking into account the hydration shell of the bilayers, which has not been treated as a separate phase so far. Various investigations have manifested the existence of a region of hydration water at the surface of the lecithin lamellae (e.g. Chapman et al., 1967; Veksli et al., 1969; Salisbury et al., 1972; Gottlieb et al., 1973). Calorimetric, X-ray, IR and NMR properties are markedly different for free water and water bound in the hydration shell. In the phase diagram of DPL/H_2O (Chapman et al., 1967), a limiting concentration appears, above which free water occurs in the gel- and in the mesomorphic lamellar state, and

above which the thermal parameters of the phase transition between these two states are no more a function of water content. All available measurements yield a mass ratio of bound water and DPL of about 20 . . 25%. For simplicity, we shall deal with a discrete 3-phase-system DPL/bound water/free water, neglecting any secondary hydration effects. Hence the indices L, B and F stand for each subsystem, respectively. All abbreviations accord to those used in sect. III.

The paramagnetic relaxation rates of the water are average values of those of free and bound water (rapid exchange case):

$$R = \frac{m_F}{m_w} R^F + \frac{m_B}{m_w} R^B, \quad (m_w = m_F + m_B),$$

or, connecting the mass of bound water to the mass of DPL by

$$m_B = p \cdot m_L,$$

we obtain

$$R = \frac{p}{M} (R^B - R^F) + R^F. \tag{12}$$

An equivalent relation holds for the diamagnetic contribution R_{dia}.

Thus the diamagnetic and paramagnetic relaxation rates are linear functions of the ratio $\frac{1}{M} = \frac{m_L}{m_w}$, as verified by the experimental data in Figure 8a and b. The slope of these straight lines is given by

$$R' = p\,(R^B - R^F). \tag{13}$$

Because all slopes are positive, we conclude that the relaxation rates in the hydration shell are enhanced both for the diamagnetic and for the paramagnetic contribution.

The enhancement of the paramagnetic contribution can principally have several reasons:

a) the effective correlation time τ_c is longer

b) the dipolar interaction between protons and oxygen is enforced by shorter distances r_{IS}

c) the oxygen concentration is higher.

We try now to rule out a) and b) and show that the reason c) is valid.

The correlation time τ_c was found to be in the range 10^{-12} to 10^{-11} s for pure water (Hausser and Noack, 1965) as well as for DPL (Kimmich and Peters, 1975). The interpretation of these extremely short correlation times was that they are determined by the spin flip fluctuation of the oxygen spin, i.e. by the electron relaxation time τ_s. The mechanism of the oxygen relaxation is the vibration modulated spin-orbit coupling within the O_2-molecule (compare Bersohn and Baird, 1966). The eigenfrequencies and the amplitudes of the vibrations are however not affected by the environment as verified by the almost identical τ_s values for oxygen in water and in DPL (Hausser and Noack, 1965; Kimmich and Peters, 1975). Thus the effective correlation time for the dipolar proton oxygen interaction can be assumed to be identical in free and bound water.

The average dipolar interaction causes perturbation fields with a distance law (Abragam, 1961)

$$\langle H_{\text{dip}}^2 \rangle \sim \frac{1}{N_H} \sum_{\text{pairs}} \frac{1}{r_{IS}^6}, \tag{14a}$$

where the sum runs over all proton-oxygen pairs. N_H is the number of protons in the water phase to be considered. The sum in Equation 14 is usually approximated by the nearest neighbour expression

$$\frac{1}{N_H} \sum_{\text{pairs}} \frac{1}{r_{IS}^6} \approx Z \frac{N_{O_2}}{N_H} \left(\frac{1}{r_{IS}^{\min}}\right)^6, \tag{14b}$$

with N_{O_2} the number of oxygen molecules and Z the coordination number of nearest neighbour protons per oxygen molecule. Keeping in mind that the repulsion energy determining the intermolecular nearest neighbour distance $r_{IS}^{\min}$ rises proportional to $\left(\frac{1}{r_{IS}^{\min}}\right)^{12}$, while the relaxation rates are only affected by the sixth power of $r_{IS}^{\min-1}$, and that the energies responsible for the formation of the hydration shell are relatively low, allows us to assume the same $r_{IS}^{\min}$ for free and bound water.

Thus the enhancement of the paramagnetic relaxation rate in the hydration shell should be due to an increased oxygen concentration, probably as a consequence of the differing water structure. This statement, however, allows to derive oxygen solubility parameters for the 3-phase-system.

Let us first define the O_2-partition-coefficients between DPL and free and bound water:

$$K_1 = \frac{C^L}{C^B}; \quad K_3 = \frac{C^L}{C^F}. \tag{15}$$

Consequently, the partition coefficient between free and bound water is

$$K_2 = \frac{C^B}{C^F} = \frac{K_3}{K_1}.$$

The argumentation presented above leads to

$$K_2 = \frac{R^B}{R^F}. \tag{16}$$

The question is now, whether K_2 is altered at the gel to liquid crystal transition.

The experimental data in Figure 8 show that the slope of the paramagnetic mass ratio curves,

$$R' = pR^F (K_2 - 1), \tag{17}$$

decreases by 9% at the phase transition. On the other hand, the paramagnetic free water rate R^F is altered by the same percentage leading to the conclusion that the alteration of R' is solely due to the decreased R^F. In other words, the quantity

$$\sigma = p (K_2 - 1) \tag{18}$$

was found to be constant. The assumption that the hydration water content p will be essentially the same in both states leads to the conclusion that K_2 is also constant. Of

course, any temperature change in principle affects the partition coefficient. However, the absolute temperature changes in our experiments only by less than 3% so that no severe effect on K_2 can be expected.

The jump coefficients for the two water phases are

$$S^B = \frac{C_0^B(45)}{C_\infty^B(37)} = \frac{R_0^B(45)}{R_\infty^B(37)} \quad \text{and} \quad S^F = \frac{C_0^F(45)}{C_\infty^F(37)} = \frac{R_0^F(45)}{R_\infty^F(37)}.$$

As a consequence of the constancy of K_2 these jump quotients turn out to be equal:

$$S^B = S^F = S. \tag{19}$$

Thus we can modify Equation 6 by

$$\Delta C_I^L = (1 - S)\{C_\infty^F(37)\frac{m^F}{m_L} + C_\infty^B(37)\frac{m^B}{m_L}\}$$

$$= C_\infty^F(37)(1 - S) \cdot (M + \sigma). \tag{20}$$

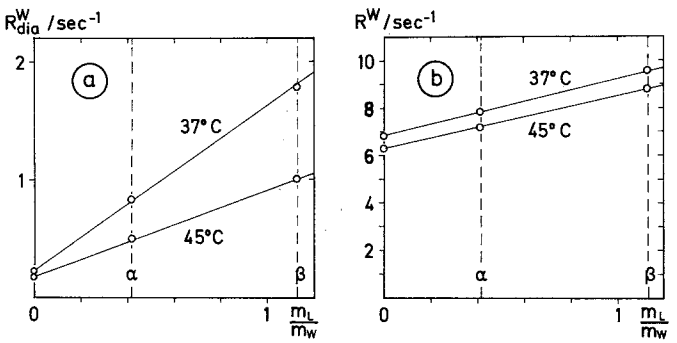

Fig. 8. Diamagnetic (**a**) and paramagnetic (**b**) water-proton relaxation rates as a function of DPL/water mass ratios. The values at $\frac{m_L}{m_w} = 0$ were measured in pure water + 0.1 m NaCl/liter

Table 2

	K_1	K_2	K_3	ΔG_1	ΔG_2	ΔG_3
37° C	0.22 . . 0.25	2.34 . . 2.67	0.58	+0.86 . . +0.94 kcal/Mol (+3.59 . . +3.93 kJ/Mol)	−0.53 . . −0.61 kcal/Mol (−2.22 . . −2.56 kJ/Mol)	+0.33 kcal/Mol (+1.4 kJ/Mol)
45° C	1.16 . . 1.32		3.09	−0.09 . . −0.17 kcal/Mol (−0.39 . . −0.74 kJ/Mol)		−0.71 kcal/Mol (−2.98 kJ/Mol)

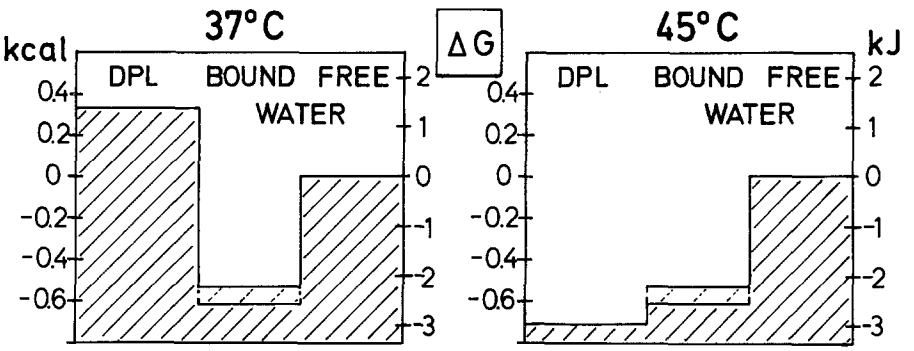

Fig. 9. The profile of the free enthalpy of oxygen solution according to the system DPL/hydration water/free water, as discussed in sect. VI. The values are presented in relation to free water

Consequently, in all expressions based on Equation 6, we have to replace M by $M + \sigma$, yielding two equations for K_3 at 37° C and 45° C analogous to Equation 7 and 8.

For the evaluation, we need the quantity $\sigma . p$ should be in the range 0.2–0.25, which was verified by diverse experimental techniques. The slope of the straight lines in Figure 8b then yields K_2 according to Equation 17. σ is calculated by the aid of Equation 18. The results are given in Table 2 and illustrated in Figure 9.

VII. Discussion of the Results and Connection to Defect Structure

In this paper we have discussed two classifications of proton phases in an aqueous DPL dispersion: one DPL phase plus one or two water phases. These distinctions have been introduced with respect to molecular motion, structural details and predominantly the different oxygen solubilities.

The distinction between free and bound water is clearly more realistic than one "average" water phase, but the corresponding treatment required a more sophisticated argumentation. So it is a matter of straightforward evidence which model is chosen. The treatment of the more complex two-phase water model is however useful in any case because it shows the degree of heterogeneity within the water phase. The most interesting point is the increased oxygen solubility in the bound water, connected with a decreased free enthalpy of solution. The explanation could be that, on the average, the structure of the hydration water offers more "vacancies" to be occupied with oxygen (compare Gottlieb et al., 1973).

One could ask whether any functional consequences for the passive transport through biological membranes can be expected from the special profile of the free enthalpy of solution Figure 9. If biological membranes are so closely adjacent to each other that their hydration shells overlap, the rate and amount of gas exchange is determined by the properties of the bound water rather than by those of the free water. An example could be stacked erythrocytes in blood.

Recently, an attempt has been made to evaluate the O_2-diffusion-constant in lipid bilayers by measuring the quenching of pyrene fluorescence in the presence of

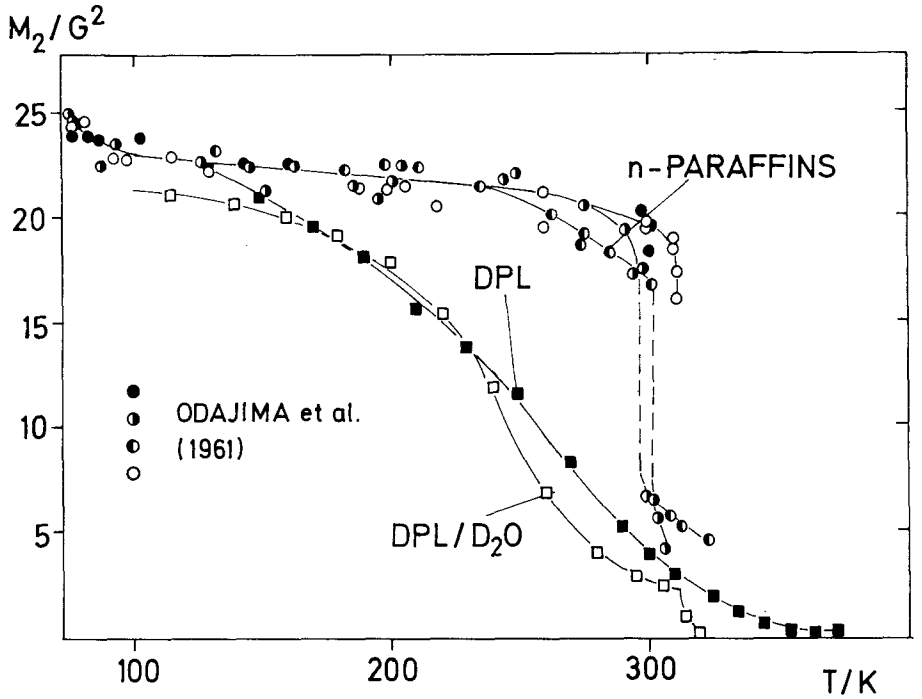

Fig. 10. Proton second moments as a function of temperature for n-$C_{18}H_{38}$ (●), n-$C_{19}H_{40}$ (◑), n-$C_{20}H_{42}$ (○), n-$C_{21}H_{44}$ (◐), powdery DPL, as purchased (■) and a homogenized but unsonicated 40% DPL/D_2O dispersion (□). ($1\ G \equiv 10^{-4}\ T$)

oxygen (Fischkoff and Vanderkooi, 1975). For these calculations, an O_2-partition-coefficient between membranes and water had to be assumed. These investigations, however, are not comparable to ours, because it is not known, in which arrangement pyrene is incorporated in the system, nor to which extent such a large molecule will cause structural and motional disturbances in the surrounding lipid phase.

It is quite clear that both models treated above are simplified because, in reality, the DPL molecules have a more heterogeneous structure than assumed. Possibly these structural details influence the oxygen solubility. A detailed study of this problem with specifically labeled lecithin is in progress. At the present state of the art, however, we have to interpret the oxygen solubility data within the DPL-bilayers as average values.

We have shown that both the gel and the liquid crystalline state of DPL bilayers as a whole dissolve oxygen to a considerable extent. What is the mechanism of solution? H. Träuble, 1971; and R. Kimmich and A. Peters, 1975, have interpreted the ability of the DPL bilayers to dissolve small molecules by assuming the formation of kink vacancies. It is well known that the liquid-crystalline state is connected with highly distorted ("fluid") alkane chain conformations which could account for the low value of the free enthalpy of solution. The gel state, however, is usually discussed in connection with completely ordered chains in the all-trans conformation, leaving no space to dissolve small molecules. Let us therefore have a look at addi-

tional experiments sensitive to the defect structure and the molecular motion within the bilayers.

Crystalline paraffins are an example for perfectly ordered all-trans chains in a virtually rigid lattice. The rigidity is demonstrated by the high value of the second moment of the proton wide-line spectrum. Odajima et al., 1962, have found values of about $25 \cdot 10^{-8}\ T^2$ (Fig. 10) compared with a theoretical value of $31 \cdot 10^{-8}\ T^2$ for a completely rigid lattice without any vibrations (Schmauder, 1976). This crystalline material dissolves no detectable amount of oxygen (Kimmich and Peters, 1975). Passing the so-called rotator phase transition activates a considerable degree of molecular motion and of the capability to dissolve oxygen. The second moment decreases to about $5 \cdot 10^{-8}\ T^2$ (Fig. 10), a value which can be explained by chain rotation and superimposed kink diffusion (Schmauder, 1976). Evidently a strong relation between chain mobility, generally connected with the formation of defects, and oxygen solubility exists.

The comparison of these results with those of the gel state of DPL bilayers shows that rotator phase paraffin is the analogous material (Fig. 10, Kimmich and Peters, 1975). The hydrocarbon chains of the DPL molecules obviously show a relatively high degree of molecular motion down to rather low temperatures. Moreover, we have found that even in solid DPL the oxygen solubility must be fairly high at temperatures where paraffins are tightly packed and unable to dissolve any detectable amount of oxygen. Of course, we cannot exclude that the oxygen molecules are incorporated in structurally caused vacancies which possibly are not affected by thermodynamics. This case should be connected with an inhomogeneous distribution of the oxygen throughout the bilayer, and should therefore be detectable with the labeled lecithin study mentioned above. In any case we can state that the hydrocarbon chains have an essentially higher degree of freedom of molecular motion than any comparable crystalline material. Finally it should be mentioned that the special properties discussed above show no abrupt alteration at the so-called pretransition.

Acknowledgements. We are grateful to Dr. K. Bergmann of BASF, Ludwigshafen for kindly providing us with the M_2 data of DPL. Several stimulating discussions with Prof. Dr. W. Pechhold are also acknowledged. This work was supported by Deutsche Forschungsgemeinschaft.

References

Abragam, A.: The principles of nuclear magnetism. Oxford: Clarendon Press 1970

Andreev, N. N., Kulikova, L. E.: K voprosu o perechode iz rastivorennogo sostojanija v dispersnoe. Žurnal obščey Chim. **5**, 366–370 (1935)

D'Ans, Lax: Taschenbuch für Chemiker und Physiker, Bd. I, 3rd Edition. Berlin-Heidelberg-New York: Springer 1967

Bersohn, M., Baird, J. C.: An introduction to electron paramagnetic resonance. New York: Benjamin 1966

Bloembergen, N., Purcell, E. M., Pound, R. V.: Relaxation effects in nuclear magnetic resonance absorption. Phys. Rev. **73**, 679–712 (1948)

Chapman, D., Williams, R. M., Ladbrooke, B. D.: Physical studies of phospholipids. VI. Thermotropic and lyotropic mesomorphism of some 1,2-diacyl-phosphatidylcholines (lecithins). Chem. Phys. Lipids **1**, 445–475 (1967)

Clare, N. D.: Supersaturation of gases in liquids. Trans. Soc. Can. [3] 19 III, 32–33 (1925)

Dost, K.: Die Löslichkeit des Luftsauerstoffs im Wasser. Mitt. Prüfungsanst. Wasserversorg. Abwässerbeseitigung (Berlin) **7,** 168–171 (1906)

Fischkoff, S., Vanderkooi, J. M.: Oxygen diffusion in biological and artificial membranes determined by the fluorochrome pyrene. J. gen. Physiol. **65,** 663–676 (1975)

Gottlieb, A. M., Inglefield, P. T., Lange, Y.: Water-lecithin binding in lecithin-water lamellar phases at 20° C. Biochim. biophys. Acta (Amst.) **307,** 444–451 (1973)

Hausser, R., Noack, F.: Kernmagnetische Relaxation und Korrelation im System Wasser-Sauerstoff. Z. Naturforsch. **20a,** 1668–1675 (1965)

Hinz, H.-J., Sturtevant, J. M.: Calorimetric studies of dilute aqueous suspensions, of bilayers formed from synthetic L-α-lecithins. J. biol. Chem. **247,** 6071–6075 (1972)

Horwitz, A. F., Michaelson, D., Klein, M. P.: Magnetic resonance studies on membrane and model membrane systems. III. Fatty acid motions in aqueous lecithin dispersions. Biochim. biophys. Acta (Amst.) **298,** 1–7 (1973)

Jackson, M. B.: A β-coupled gauche kink description of the lipid bilayer phase transition. Biochemistry **15,** 2555–2561 (1976)

Kimmich, R.: Consequences of restricted defect diffusion on NMR and dielectric relaxation. Z. Naturforsch. **31a,** 693–696 (1976)

Kimmich, R., Peters, A.: Defect diffusion in crystalline lipid lamellae and nuclear magnetic relaxation behaviour. J. Magnetic Resonance **19,** 144–165 (1975)

Kimmich, R., Peters, A.: Solvation of oxygen in lecithin bilayers. Chem. Phys. Lipids **14,** 350–362 (1975)

Krause, A., Kapitańczyk, K.: Über kolloide Gase. III. Kolloide Luft und kolloider Sauerstoff mit einer Bläschengröße von 5 μμ bzw. 3 μμ Teilchendurchmesser. Kolloid-Z. **71,** 55–60 (1935)

Odajima, A., Sauer, J. A., Woodward, A. E.: Proton magnetic resonance of some normal paraffins and polyethylene. J. Phys. Chem. **66,** 718–724 (1962)

Pechhold, W.: Molekülbewegung in Polymeren. I. Teil: Konzept einer Festkörperphysik makromolekularer Stoffe. Kolloid-Z. Z. Polymere **228,** 1–38 (1968)

Metschl, J.: The supersaturation of gases in water and certain organic liquids. J. Phys. Chem. **28,** 417–437 (1924)

Salsbury, N. J., Darke, A., Chapman, D.: Deuteron magnetic resonance studies of water associated with phospholipids. Chem. Phys. Lipids **8,** 142–151 (1972)

Schmauder, K.: Untersuchungen zum 2. Moment und zur Linienform der Kernresonanzabsorptionslinien von Polyäthylen mit der Impulsmethode. Ulm: Diplomarbeit 1976

Seelig, A., Seelig, J.: The dynamic structure of fatty acyl chains in a phospholipid bilayer measured by deuterium magnetic resonance. Biochemistry **13,** 4839–3844 (1974)

Träuble, H.: Phase transitions in lipids. In: Biomembranes, vol. 3. Passive permeability of cell membranes (eds. F. Kreuzer, J. F. G. Slegers). New York-London: Plenum Press 1972

Träuble, H.: The movement of molecules across lipid membranes: A molecular theory. J. Membrane Biol. **4,** 193–208 (1971)

Träuble, H., Eibl, H.: Cooperative structural changes in lipid bilayers. In: Functional linkage in biomolecular systems, Chapt. III. Molecular interactions in lipid bilayers (eds. F. O. Schmitt, D. M. Schneider, D. M., Crothers). New York: Raven Press 1975

Veksli, Z., Salsbury, N. J., Chapman, D.: Physical studies of phospholipids. XII. Nuclear magnetic resonance studies of molecular motion in some pure lecithin-water systems. Biochim. biophys. Acta (Amst.) **183,** 434–446 (1969)

Zimmerman, J. R., Brittin, W. E.: Nuclear magnetic-resonance studies in multiple phase systems: Lifetime of a water molecule in an adsorbing phase on silica gel. J. Phys. Chem. **61,** 1328–1333 (1957)

Received January 21, 1977/Accepted June 8, 1977